

1 **Title**

2 Characterization of three tissue fractions in corn (*Zea mays*) cob

3

4 **Authors**

5 Masatsugu Takada, Rui Niu, Eiji Minami, Shiro Saka*

6 Department of Socio-environmental Energy Science, Graduate School of Energy

7 Science, Kyoto University, Yoshida-honmachi, Sakyo-ku, Kyoto 806-8501, Japan

8 * Corresponding author. E-mail: saka@energy.kyoto-u.ac.jp

9

10 **Keywords**

11 microscopic observation; cinnamic acids; hemicellulose; lignin; tissue fractions

12

13

14

15 **Abstract**

16

17 Corn (*Zea mays*) cob is composed of three tissue fractions: chaff (21.1%), woody ring
18 (77.5%) and pith (1.4%). In this study, the cell wall components in these tissue fractions
19 were characterized so as to examine their tissue morphology. As a result, it was found that
20 the chemical compositions in three fractions were relatively similar, and the hemicellulose
21 was the main component. Through their sugar composition analysis, hemicellulose was
22 mainly composed of xylan in all fractions, while the proportion of arabinose and galactose
23 was different in the woody ring, compared with other two fractions. From the alkaline
24 nitrobenzene oxidation analysis, lignin in all fractions was composed all of guaiacyl,
25 syringyl and *p*-hydroxyphenyl lignins, while their ratios varied in three fractions.
26 Furthermore, the amounts of cinnamic acids such as ferulic and *p*-coumaric acids, which
27 are associated with the corn lignin, were also different among three fractions. With respect
28 to the tissue morphology, the component cells in three fractions were totally different each
29 other. Furthermore, from the ultraviolet microspectrophotometry of each morphological
30 region in three tissue fractions, it was found that the lignin concentration and distribution

31 of cinnamic acids were different from one morphological region to another. These kinds
32 of information would provide a clue as to efficient utilization of corn cob into value-added
33 chemicals.

34

35

36 **1. Introduction**

37

38 Corn (*Zea mays*) is the most produced foodstuff in the world like the sugarcane [1]. As a
39 by-product of the corn production, corn cob is estimated to be produced with the yield of
40 164 million Mg all over the world [2]. For its utilization, various researches have been
41 conducted to produce valuable chemicals such as xylitol [3,4], ethanol [3,5–10] and
42 cellulose nanofibers [11–13]. For the practical production, corn cob has been used as a
43 resource for bioethanol production in China since 2013 [14]. In order to utilize the
44 lignocellulosics for biofuels or chemicals, it is quite essential to understand its chemical
45 characteristics and structures.

46 The cell walls of the lignocellulosics are mainly composed of cellulose,
47 hemicellulose and lignin, and their components and compositions are different depending
48 on the lignocellulosic species [15]. For the whole corn cob, several researchers have
49 studied its chemical structures, especially for hemicellulose [9,16,17]. On the other hand,
50 the corn cob is composed of three tissue fractions: chaff, woody ring and pith [18]. The
51 shapes, densities and physical structures are totally different among the three fractions,

52 while their detailed chemical structures were not characterized yet.

53 In this study, thus, the chemical compositions and the characteristics of the main
54 cell wall components such as cellulose, hemicellulose and lignin, were examined for the
55 separated three tissue fractions of the corn cob. Furthermore, their component cells and
56 the distributions of lignin including cinnamic acids were examined with ultraviolet
57 microspectrophotometry.

58

59

60 2. Materials and methods

61

62 2.1. Samples and chemicals

63

64 Corn used in this study was harvested in Langfang city, Habei province, China. The
65 sampling time and sample age were April 2015 and 0.4 years, respectively. The storage
66 temperature and humidity before delivery to the laboratory were 10-20°C and 60-70%,
67 respectively. The sample condition during delivery was air-dried and the corn cob was
68 separated from grans before the delivery. These information was shown in accordance
69 with the checklist for sample definition by Barton [19]. Upon arrival in the laboratory,
70 three different tissue fractions (outer part, chaff; middle part, woody ring; inner part, pith)
71 were separated by using a knife as shown in Fig. 1, and the separated fractions were dried
72 at 105°C for 12 h to measure their oven-dried weight. The fractionated samples were then
73 milled in a small grinder (Wonder Blender WB-1: Osaka chemical Co., Ltd., Osaka,
74 Japan), and used for various analyses. The analyses described below were conducted at
75 least 3 times and the average values were used. The chemicals used in this study were of

76 reagent grade without any purification, purchased from Nacalai Tescque, Inc., Kyoto,
77 Japan. The unit “%” used in this paper is based on weight.

78 --- (Fig. 1) ---

79

80

81 2.2. Analytical methods

82

83 Chemical compositions in three tissue fractions were evaluated using the method of
84 Rabemanolontsoa et al. [20].

85 X-ray diffractograms were obtained by Rigaku RINT 2,200V (Rigaku Corp., Tokyo,
86 Japan) with Ni-filtered Cu-K α radiation ($\lambda = 0.1542$ nm) generated at 40 kV and 30 mA
87 to evaluate the crystalline structure of cellulose, according to the ordinary method for
88 holocellulose production [21]. The crystallinity index is estimated according to the
89 calculation methods by Segal et al. as shown below [22].

90

91
$$\text{CrI} = \frac{I_{002} - I_{\text{am}}}{I_{002}} \times 100$$

92

93 I_{002} is the maximum intensity of the 002 lattice diffraction at $2\theta = 22.5^\circ$, and I_{am} is the
94 intensity of the diffraction at $2\theta = 18.0^\circ$.

95

96 The composition of hemicellulosic saccharides was determined using the acid
97 methanolysis method [23], and the obtained monosaccharides were quantified by gas
98 chromatography-mass spectrometry (GC-MS) analysis using GCMS-QP 2010 Ultra
99 (Shimadzu Co., Kyoto, Japan) after the trimethylsilyl derivatization [2]. Furthermore,
100 acetic acid content was analyzed using the acid hydrolysis method with 72% H_2SO_4
101 followed by 3% H_2SO_4 [24]. Subsequently, the obtained hydrolyzates were analyzed with
102 high performance liquid chromatography (HPLC) (LC-10A, Shimadzu Co., Kyoto,
103 Japan) [2].

104 For the analysis of the lignin structure, the alkaline nitrobenzene oxidation was
105 performed according to the ordinary method and the total yields of vanillin,
106 syringaldehyde, and *p*-hydroxybenzaldehyde were determined by gas chromatography
107 (GC: GC 2014, Shimadzu Co., Kyoto, Japan) [25]. The vanillin and *p*-

108 hydroxybenzaldehyde can be produced from ferulic acid and *p*-coumaric acid,
109 respectively, since both acids were associated with corn lignin [26–30]. Thus, the yields
110 of cinnamic acids-derived vanillin and *p*-hydroxybenzaldehyde were subtracted from the
111 original yield of the alkaline nitrobenzene oxidation products to obtain the actual yields
112 of products from lignin.

113 As described above, the corn lignin contained some cinnamic acids such as ferulic
114 acid (4-hydroxy-3-methoxycinnamic acid) and *p*-coumaric acid (4-hydroxycinnamic
115 acid). The fractionated flour was treated with 0.5 mol L⁻¹ NaOH to extract the cinnamic
116 acids [31]. The extracted portion was acidified with dilute HCl and then extracted with
117 ethyl acetate. The ethyl acetate-soluble portion was then dehydrated and evaporated under
118 vacuum. The obtained products were trimethylsilyl derivatized followed by GC-MS
119 analysis [32].

120

121

122 2.3. Microscopic observations

123

124 The distribution of lignin including cinnamic acids were observed by UV microscopy
125 [33]. Each tissue fraction was embedded in epoxy resin, and the samples were cut into
126 0.5 μm thick section with a diamond knife mounted on a Leica Reichert Supernova
127 Microtome (Buffalo Grove, IL, USA). The sections were placed on the quartz slides,
128 mounted with glycerin and covered with quartz coverslip before examination by MSP-
129 800 system (Carl Zeiss, Oberkochen, Germany) with a specified filter at $280\text{ nm} \pm 5\text{ nm}$.
130 The morphological regions of the each fraction were analyzed on a UV
131 microspectrophotometry based on photometric point-by-point measurements (spot size:
132 $1\ \mu\text{m} \times 1\ \mu\text{m}$).

133

134

135 **3. Results and discussions**

136

137 **3.1. Characteristics and chemical compositions of three tissue fractions**

138

139 The images of three tissue fractions of corn cob and their dried weight compositions are
140 shown in Fig. 1. The corn cob is composed of three tissue fractions whose physical
141 structures are different one another. The outer part, chaff, is light and stiff, and its structure
142 is wrinkled. The middle part, woody ring, is a lignified structure and very stiff like a
143 woody xylem. The inner part, pith, is extremely light and its structure is spongy. The chaff,
144 woody ring and pith account for 21.1%, 77.5% and 1.4%, respectively.

145 The chemical compositions in three tissue fractions are presented in Table 1.
146 Hemicellulose is the main component in all fractions, especially in the woody ring with
147 46.9%. Cellulose is the second largest component, next to the hemicellulose, and the
148 proportion of the holocellulose (cellulose + hemicellulose) is quite high in all regions. On
149 the other hand, the lignin content is less than 20% in all fractions, smaller than that of
150 woody biomass. Although the woody ring sounds to be high in lignin content, its content
151 is, in fact, lower than other two fractions. For the extractives, the pith contained 3.5%,
152 which is the highest among three fractions. The ash content is the highest in the chaff and
153 the lowest in the woody ring. Accordingly, there are some differences in the chemical
154 composition between three tissue fractions, while their overall compositions are relatively

155 similar. Since each component was quantified independently, the total values are not
156 necessary equal to 100%. However, it was not adjusted.

157 For the further characterization, the detailed analyses of the main cell wall
158 components such as cellulose, hemicellulose and lignin were conducted for three fractions.

159 --- (Table 1) ---

160

161

162 3.2. Structure of each cell wall component of three tissue fractions

163

164 3.2.1. Cellulose

165

166 In order to examine the crystalline structure of cellulose in three fractions, X-ray
167 diffractometric (XRD) analysis was performed and Fig. 2 shows the X-ray diffractograms
168 of the holocellulose (cellulose + hemicellulose) obtained from three morphological
169 regions. Their XRD patterns are relatively similar. The XRD intensity of the pith is lower
170 than those of other two fractions, due perhaps to its quite low density. The crystallinity

171 indexes of their holocelluloses are calculated according to the methods of Segal et al. and
172 shown in Fig. 2. As a result, the crystallinity index of holocellulose from woody ring
173 (42.4) is the highest, compared with those of chaff (39.9) and pith (38.5), but their
174 crystallinity indexes are quite similar, indicating that their structures of crystalline
175 cellulose are relatively similar.

176 --- (Fig. 2) ---

177

178

179 3.2.2. Hemicellulose

180

181 The hemicellulosic sugar compositions in three tissue fractions are presented in Table 2.

182 Xylose is the main sugar components in all fractions. Among three fractions, the woody

183 ring contained higher proportion of xylose, while its arabinose and galactose contents are

184 much lower compared to the chaff and pith. As to the uronic acids, both glucuronic acid

185 and 4-*O*-methyl glucuronic acid are obtained from the chaff and pith, while for woody

186 ring, 4-*O*-methyl glucuronic acid was not detected. Accordingly, the hemicellulosic sugar

187 components are the same in three fractions except for 4-*O*-methyl glucuronic acid,
188 whereas their sugar compositions are different among three fractions.

189 In addition, the acetic acid, which is considered to be derived from the acetyl residue,
190 are obtained from all fractions. Their yields in chaff, woody ring and pith are 2.8%, 4.7%
191 and 4.4%, respectively.

192 ---(Table 2)---

193

194

195 3.2.3. Lignin

196

197 For the structural analysis of lignin, the alkaline nitrobenzene oxidation was performed
198 for three tissue fractions, and the results are shown in Fig. 3. As the decomposed products
199 from guaiacyl (G), syringyl (S) and *p*-hydroxyphenyl (H) lignins, vanillin,
200 syringaldehyde and *p*-hydroxybenzaldehyde are obtained, respectively. In case of the corn
201 lignin, the cinnamic acids such as ferulic acid and *p*-coumaric acid are associated with
202 lignin as described above. By the alkaline nitrobenzene oxidation, the ferulic acid and *p*-

203 coumaric acid can be converted into the vanillin and *p*-hydroxybenzaldehyde,
204 respectively. Thus, the yields of the decomposed products from lignin were evaluated
205 from the total yields of decomposed products minus the yields of decomposed products
206 from cinnamic acids. As a result, all of three decomposed products were obtained from
207 all tissue fractions, indicating that lignin in three fractions are composed all of G, S and
208 H lignins. The yields of the decomposed products are highest in the woody ring and the
209 lowest in the chaff. For all fractions, vanillin is the main products, while the ratios of
210 syringaldehyde and *p*-hydroxybenzaldehyde are different among three fractions,
211 indicating that the compositions of G, S and H lignins would be different from one tissue
212 fraction to another.

213 --- (Fig. 3) ---

214 Table 3 shows the yields of ferulic acid and *p*-coumric acid in three tissue fractions
215 as determined by the aqueous alkali treatment. As a result, both yields are different in
216 three tissue fractions. The content of ferulic acid in the woody ring is lower than that in
217 the chaff and pith. In herbaceous plants, ferulic acid is associated with lignin and
218 hemicellulose via ester and ether linkages as bridges between lignin and hemicellulose,

219 forming lignin/phenolics - carbohydrate complexes (LCC) [34], and the ferulic acid
220 esterified the *O*-5 position of α -L-arabinofuranosyl residues of arabinoxylan [26–29]. Fig.
221 4 shows the correlation between ferulic acid and arabinose contents in three tissue
222 fractions. The woody ring, whose ferulic acid content is the lowest, contains the lowest
223 arabinose content among three fractions. The positive correlation between ferulic acid
224 and arabinose contents would be due to the LCC linkages between them. It is interesting
225 that the woody ring contains high hemicellulose content, while low arabinose and ferulic
226 acid contents, indicating that the woody ring would contain less LCC structure compared
227 to other fractions.

228 --- (Table 3) ---

229 --- (Fig. 4) ---

230 With respect to the *p*-coumaric acid, in case of the corn stover, the *p*-coumaric acid
231 is associated with S lignin at γ position of propane side-chain according to the 2D-NMR
232 analysis [30]. Fig. 5 shows the correlation between the *p*-coumaric acid content and
233 syringaldehyde obtained by alkaline nitrobenzene oxidation in three tissue fractions.
234 Given that the syringaldehyde is obtained from S lignin, its yield can be an indicator to

235 evaluate the ratio of S lignin. As a result, woody ring, whose *p*-coumaric acid content is
236 the highest, produces the highest yields of syringaldehyde compared to other fractions.
237 Accordingly, the *p*-coumaric acid might associate with S lignin as well as corn stover.
238 However, further experiments should be required to discuss the detailed chemical
239 structures.

240 --- (Fig. 5) ---

241

242

243 3.3. UV microscopy of three tissue fractions

244

245 Fig. 6 shows the ultraviolet (UV) micrographs of three tissue fractions taken at a
246 wavelength of 280 nm. Among the cell wall components, only lignin can absorb UV light
247 due to its aromatic structure. Thus, the darker area in UV micrographs shows the higher
248 concentration of lignin to be blacker. The three tissue fractions are composed of different
249 types of cells.

250 --- (Fig. 6) ---

251 The chaff is composed of sclerenchyma cells and their structures are wrinkled (Fig.
252 6 (a)). The middle lamella portion shows blacker compared to the cell wall portion,
253 indicating that the lignin concentration in the middle lamella would be higher than that in
254 the cell wall.

255 The woody ring is composed of vascular bundle and parenchyma cells as shown
256 in Fig. 6 (b-1) and (b-2), respectively. The vascular bundle region is composed of various
257 kinds of cells such as fiber, vessel and sieve tube. Compared to the parenchyma region,
258 the vascular bundle region shows blacker, which indicates that the lignin concentration of
259 vascular bundle region would be higher than that of parenchyma region. As well as the
260 chaff, the middle lamella portion is higher in its lignin concentration compared to the cell
261 wall portion.

262 Regarding the pith (Fig. 6 (c)), the size of component cell is quite large with an
263 average diameter of 100 μm and all of them are parenchyma cells. Air spaces are often
264 observed between the adjacent cells.

265 For more detailed analysis of the lignin distribution in the three tissue fractions,
266 the UV microspectrophotometry was performed for each morphological region, and the

267 results are shown in Fig. 7. As for the sclerenchyma cells in chaff (Fig. 7 (a)), the cell
268 wall (CW) and the middle lamella at cell corner (ML_{CC}) shows the highest peak at a
269 wavelength of 323 nm and 318 nm, respectively. In case of the ordinary woody biomass,
270 both the secondary wall and the middle lamella show the peak at a wavelength of 275~280
271 nm [35,36]. According to the experiments with the model compounds, it was found that
272 the ethyl-ferulate and ethyl-*p*-coumarate showed the peak at a wavelength of 325 nm and
273 313 nm, respectively [37]. Thus, it would be more likely that the shift of peak wavelength
274 from 280 nm to 320 nm is due to the association of cinnamic acids to corn lignin.
275 Accordingly, the difference in the wavelength of peak between CW and ML_{CC} would
276 indicate that the CW contains more ferulic acid compared to *p*-coumaric acid, while ML_{CC}
277 contains more *p*-coumaric acid compared to ferulic acid. Therefore, the distribution of
278 cinnamic acids would be different from one morphological region to another.

279 --- (Fig. 7) ---

280 For the woody ring, the UV spectra of the vessel, the sieve tube, the fiber and the
281 parenchyma are shown in Fig. 7 (b-1, b-2). Since the cell walls of fiber and parenchyma
282 have enough thickness to determine the UV spectra (1 $\mu\text{m} \times 1 \mu\text{m}$), their CW and ML_{CC}

283 regions were separately determined. All spectra showed the peak at a wavelength of
284 around 320 nm as well as those of chaff. The UV spectra of vessel and parenchyma
285 showed the highest absorbance at 315 nm, while those of fiber showed at 325 nm for both
286 CW and ML_{CC} portions. Such results would indicate that the fiber contained more ferulic
287 acid compared to *p*-coumaric acid, while the vessel and parenchyma contained more *p*-
288 coumaric acid.

289 For the pith, UV microspectrophotometry analysis was performed not for each
290 morphological region, since the cell wall and middle lamella can not be distinguished due
291 to the thin cell wall and there are no ML_{CC} due to the air spaces. As a result, the highest
292 UV absorbance was obtained at a wavelength of 320 nm as well as other two fractions.

293 From the UV spectrophotometric analysis, it was found that cinnamic acids are
294 not uniformly distributed in three tissue fractions and their distributions are different from
295 one morphological region to another. However, further experiments would be required to
296 discuss the quantitative evaluation of the distribution of lignin including cinnamic acids.

297

298 **Conclusions**

299

300 The characterization of chemical structures was performed for three tissue fractions of
301 corn (*Zea mays*) cob; chaff, woody ring and pith. As a result, the chemical compositions
302 in three fractions were relatively similar, and the hemicellulose was the main component
303 in all fractions. With respect to the hemicellulosic sugar, the woody ring contained higher
304 xylose and lower of arabinose and galactose compared to chaff and pith. From the alkaline
305 nitrobenzene oxidation, the compositions of G, S and H lignins would be different from
306 one tissue fraction to another. As for the cinnamic acids, the woody ring contained lower
307 furulic acid and higher of *p*-coumaric acid compared to other fractions. The ferulic acid
308 content has a positive correlation with arabinose content, and *p*-coumaric acid with
309 syringaldehyde yields by nitrobenzene oxidation. These positive correlations would indicate
310 their chemical structures in corn cob.

311 From the UV microspectrophotometry analysis, the component cells were totally
312 different in three tissue fractions and the lignin concentration and the distribution of
313 cinnamic acids were different from one morphological region to another.

314 The differences of chemical composition and lignin structures in lignocellulosics
315 influence on its decomposition behaviors in various kind of treatments. Furthermore, the
316 distribution of lignin also has an impact on the delignification behaviors. Accordingly,
317 these results obtained in this study are quite important to understand the decomposition
318 behaviors of corn cob in various decomposition treatments. Thus, such information would
319 provide a clue as to efficient utilization of corn cob for biofuels or biochemicals.

320

321

322

323 **Acknowledgements**

324

325 This work was supported by the Japan Science and Technology Agency (JST) under the
326 Advanced Low Carbon Technology Research and Development Program (ALCA) and
327 Kakenhi (No. 16J11212) a Grant-in-Aid for Japan Society for the Promotion of Science
328 (JSPS) fellow, for which the authors are extremely grateful.

329

330 **References**

331

332 [1] World Agricultural Production, Production, supply and distribution, 2016.

333 <http://apps.fas.usda.gov/psdonline/>

334 [2] M. Takada, R. Niu, E. Minami, S. Saka, Two-step hydrolysis of corn (*Zea mays*)

335 cobs treated with semi-flow hot-compressed water, *Int. J. Agric. Crop Sci.* (2017).

336 (in press)

337 [3] F. Latif, M.I. Rajoka, Production of ethanol and xylitol from corn cobs by yeasts

338 *Bioresource Technology*, *Bioresour. Technol.* 77 (2001) 57–63.

339 [4] H. Ling, K. Cheng, J. Ge, W. Ping, Statistical optimization of xylitol production

340 from corncob hemicellulose hydrolysate by *Candida tropicalis* HDY-02, *N.*

341 *Biotechnol.* 28 (2011) 673–678.

342 [5] D.S. Beall, L.O. Ingram, A. Ben-Bassat, J.B. Doran, D.E. Fowler, R.G. Hall, B.E.

343 Wood, Conversion of hydrolysates of corn cobs and hulls into ethanol by

344 recombinant *Escherichia coli* B containing integrated genes for ethanol production,

345 *Biotechnol. Lett.* 14 (1992) 857–862.

- 346 [6] H.G. Lawford, J.D. Rousseau, Fuel ethanol from corn residue prehydrolysate by a
347 patented ethanologenic *Escherichia coli* B, *Biotechnol. Lett.* 14 (1992) 421–426.
- 348 [7] M. Chen, L. Xia, P. Xue, Enzymatic hydrolysis of corncob and ethanol production
349 from cellulosic hydrolysate, *Int. Biodeterior. Biodegrad.* 59 (2007) 85–89.
- 350 [8] K. Liu, X. Lin, J. Yue, X. Li, X. Fang, M. Zhu, J. Lin, Y. Qu, L. Xiao, High
351 concentration ethanol production from corncob residues by fed-batch strategy,
352 *Bioresour. Technol.* 101 (2010) 4952–4958.
- 353 [9] D. Van Eylen, F. van Dongen, M. Kabel, J. de Bont, Corn fiber, cobs and stover:
354 Enzyme-aided saccharification and co-fermentation after dilute acid pretreatment,
355 *Bioresour. Technol.* 102 (2011) 5995–6004.
- 356 [10] Y. Chen, B. Dong, W. Qin, D. Xiao, Xylose and cellulose fractionation from
357 corncob with three different strategies and separate fermentation of them to
358 bioethanol, *Bioresour. Technol.* 101 (2010) 6994–6999.
- 359 [11] S. Kumar, Y.S. Negi, J.S. Upadhyaya, Studies on characterization of corn cob
360 based nanoparticles, *Adv. Mater. Lett.* 1 (2010) 246–253.
- 361 [12] M. Li, Y.L. Cheng, N. Fu, D. Li, B. Adhikari, X.D. Chen, Isolation and

- 362 characterization of corncob cellulose fibers using microwave-assisted chemical
363 treatments, *Int. J. Food Eng.* 10 (2014) 427–436.
- 364 [13] R.L. Shogren, S.C. Peterson, K.O. Evans, J.A. Kenar, Preparation and
365 characterization of cellulose gels from corn cobs, *Carbohydr. Polym.* 86 (2011)
366 1351–1357.
- 367 [14] J. Clever, A. Anderson-specher, J. Jiang, China - Peoples republic of biofuels
368 annual China's 2014 fuel ethanol production is forecast to increase six percent,
369 USDA Foreign Agricultural Serv. (2014).
- 370 [15] H. Rabemanolontsoa, S. Saka, Comparative study on chemical composition of
371 various biomass species, *RSC Adv.* 3 (2013) 3946-3956.
- 372 [16] F.E.M. Van Dongen, D. Van Eyllen, M.A. Kabel, Characterization of substituents
373 in xylans from corn cobs and stover, *Carbohydr. Polym.* 86 (2011) 722–731.
- 374 [17] Z. Hromádková, J. Kováčiková, A. Ebringerová, Study of the classical and
375 ultrasound-assisted extraction of the corn cob xylan, *Ind. Crops Prod.* 9 (1999)
376 101–109.
- 377 [18] E. Lathrop, J. Shollenberger, Corn cobs - their composition, availability, farm and

- 378 industrial uses, Illinois, (1947).
- 379 [19] G.M. Barton, Definition of biomass samples involving wood, bark and foliage,
380 Biomass 4 (1984) 311-314.
- 381 [20] H. Rabemanolontsoa, S. Ayada, S. Saka, Quantitative method applicable for
382 various biomass species to determine their chemical composition, Biomass and
383 Bioenergy. 35 (2011) 4630–4635.
- 384 [21] L.E. Wise, M. Maxine, A.A. D’Addieco, Chlorite holocellulose, its fractionation
385 and bearing on summative wood analysis and on studies on the hemicelluloses,
386 Tech. Assoc. Pulp Pap. Ind. 29 (1946) 210–218.
- 387 [22] L. Segal, J.J. Creely, A.E. Martin, C.M. Conrad, An empirical method for
388 estimating the degree of crystallinity of native cellulose using the X-ray
389 diffractometer, Text. Res. J. 29 (1959) 786–794.
- 390 [23] F. Bertaud, A. Sundberg, B. Holmbom, Evaluation of acid methanolysis for
391 analysis of wood hemicelluloses and pectins, Carbohydr. Polym. 48 (2002) 319–
392 324.
- 393 [24] C.W. Dence, The Determination of Lignin, in: S.Y. Lin, C.W. Dence (Eds.),

- 394 Methods in Lignin Chemistry, Springer Verlag, Berlin, 1992, pp. 33–58.
- 395 [25] C.-L. Chen, Nitrobenzene and cupric oxide oxidations, in: S.Y. Lin, C.W. Dence
396 (Eds.), Methods in Lignin Chemistry, Springer Verlag, Berlin, 1992, pp. 301–321.
- 397 [26] E. Allerdings, J. Ralph, H. Steinhart, M. Bunzel, Isolation and structural
398 identification of complex feruloylated heteroxylan side-chains from maize bran,
399 Phytochemistry. 67 (2006) 1276–1286.
- 400 [27] C.B. Faulds, G. Williamson, The role of hydroxycinnamates in the plant cell wall,
401 J. Sci. Food Agric. 79 (1999) 393–395.
- 402 [28] T. Ishii, Structure and functions of feruloylated polysaccharides, Plant Sci. 127
403 (1997) 111–127.
- 404 [29] T.W. Jeffries, Biodegradation of lignin and hemicelluloses, in: C. Ratledge (Ed.),
405 Biochem. Microb. Degrad., Springer Netherlands, Netherlands, 1994, pp. 233–277.
- 406 [30] J. Grabber, S. Quideau, J. Ralph, *p*-Coumaroylated syringyl units in maize lignin:
407 Implications for β -ether cleavage by thioacidolysis, Phytochem. 43 (1996) 1189–
408 1194.
- 409 [31] P. Torre, B. Aliakbarian, B. Rivas, J.M. Dominguez, A. Converti, Release of

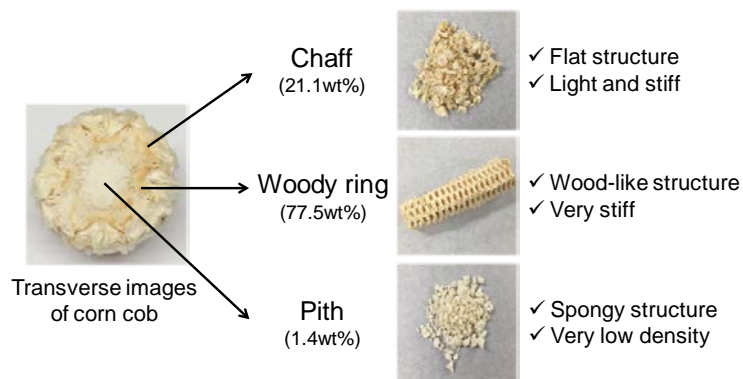
- 410 ferulic acid from corn cobs by alkaline hydrolysis, *Biochem. Eng. J.* 40 (2008)
411 500–506.
- 412 [32] M. Takada, S. Saka, Characterization of lignin-derived products from Japanese
413 cedar as treated by semi-flow hot-compressed water, *J. Wood Sci.* 61 (2015) 299–
414 307.
- 415 [33] M. Takada, S. Saka, Comparative study on topochemistry of delignification from
416 Japanese cedar and Japanese beech by hydrothermal treatment, *J. Wood Sci.* 61
417 (2015) 602–607.
- 418 [34] T. Higuchi, Y. Ito, M. Shimada, I. Kawamura, Chemical properties of milled wood
419 lignin of grasses, *Phytochemistry.* 6 (1967) 1551–1556.
- 420 [35] B.J. Fergus, D.A.I. Goring, The location of guaiacyl and syringyl lignins in birch
421 xylem tissue, *Holzforschung.* 24 (1970) 113–117.
- 422 [36] B.J. Fergus, A.R. Procter, J.A.N. Scott, D.A.I. Goring, The distribution of lignin
423 in sprucewood as determined by ultraviolet microscopy, *Wood Sci. Technol.* 3
424 (1969) 117–138.
- 425 [37] L. He, N. Terashima, Formation and structure of lignin in monotyledons II.

426 Deposition and distribution of phenolic acids and their association with cell wall

427 polymers in rice plants (*Oryza sativa*), Mokuzaigakkaishi. 35 (1989) 123–129.

428

429

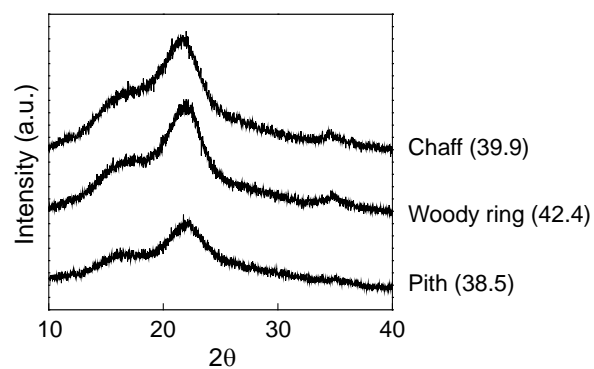


430

431

Fig. 1 Three tissue fractions of corn cob

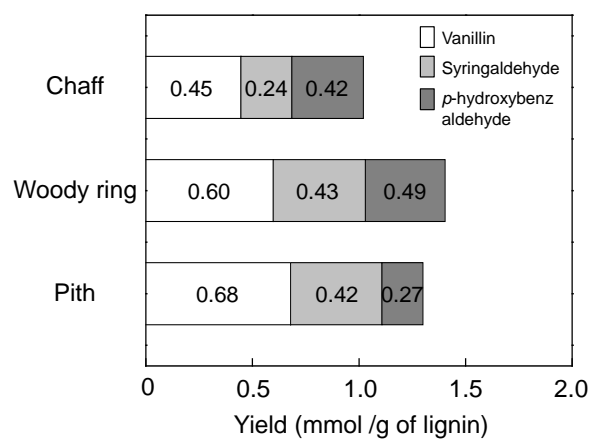
432



433

434 Fig. 2 XRD spectra of three tissue fractions of corn cob. The numbers in parenthesis
435 indicate the crystallinity indexes.

436

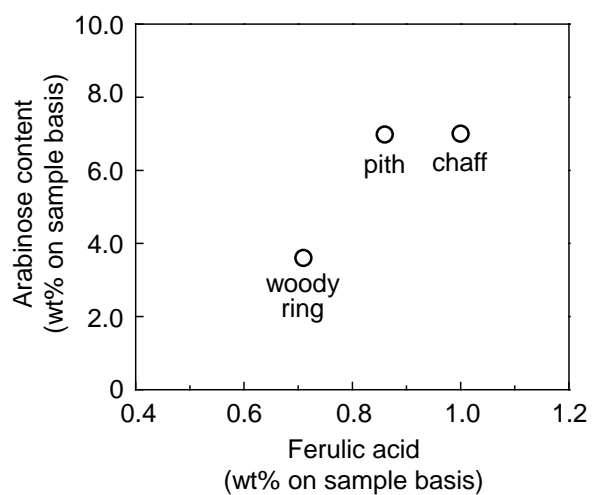


437

438 Fig. 3 Yield of alkaline nitrobenzene oxidation products for three tissue fractions of corn
439 cob

440

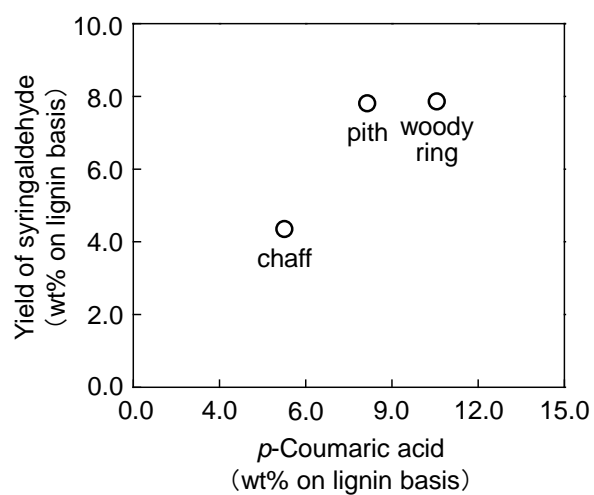
441



442

443 Fig. 4 Correlation between ferulic acid and arabinose contents in three tissue fractions of
444 corn cob

445



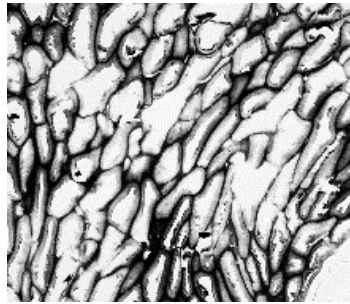
446

447 Fig. 5 Correlation between *p*-coumaric acid and the yield of syringaldehyde obtained by

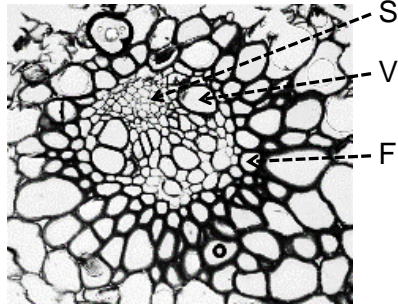
448 alkaline nitrobenzene oxidation in three tissue fractions of corn cob

449

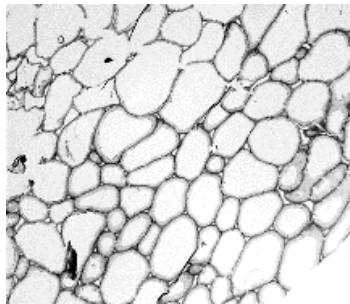
450



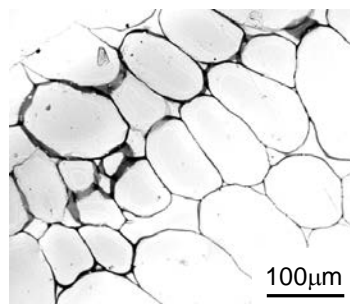
(a) Chaff



(b-1) Woody ring
(Vascular bundle)



(b-2) Woody ring
(Parenchyma)



(c) Pith

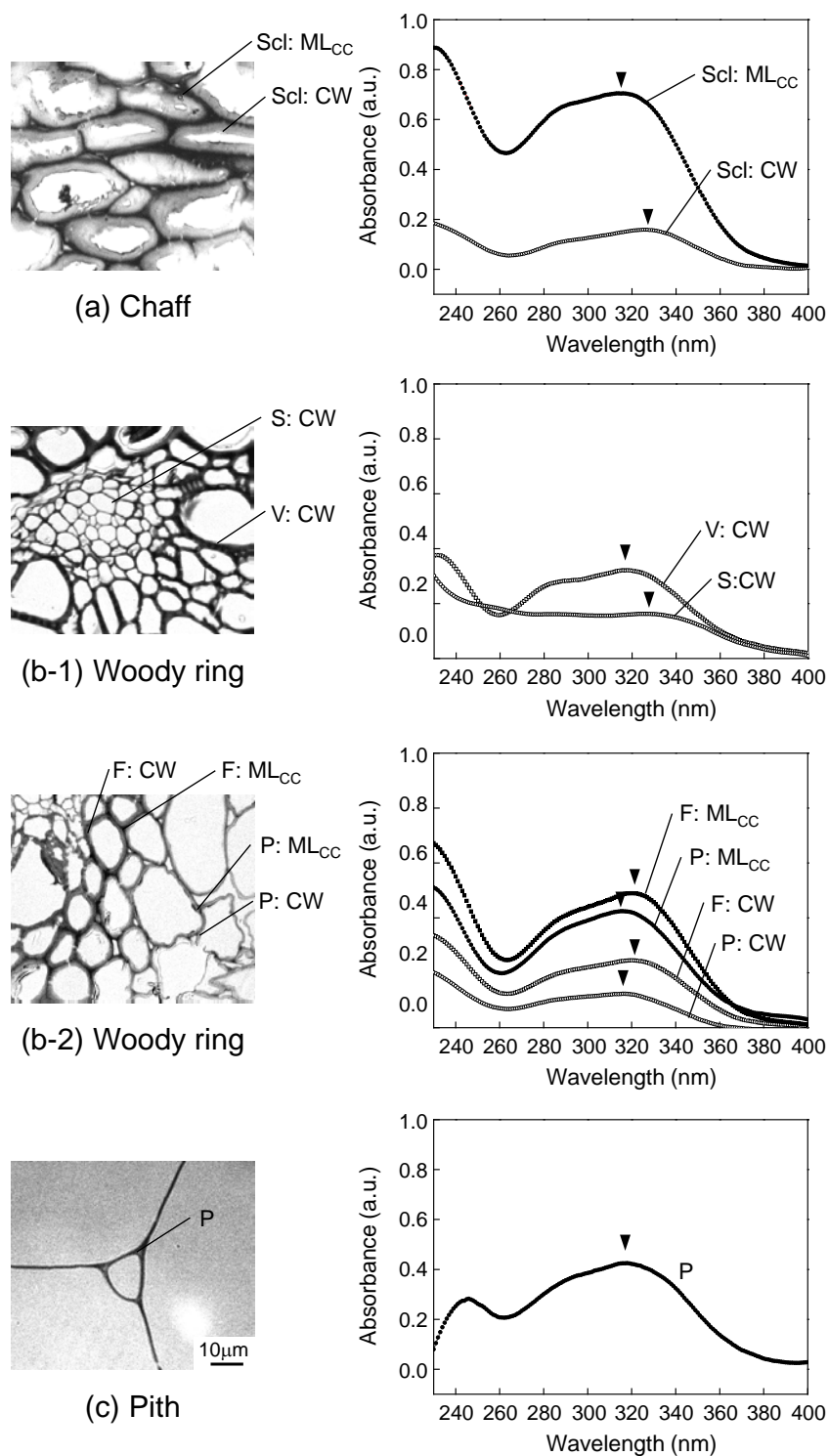
451

452 Fig. 6 UV micrographs of three tissue fractions at a wavelength of 280 nm. S: sieve tube,

453 V: vessel, F: fiber

454

455



456

457 Fig. 7 UV micrographs of three tissue fractions taken at a wavelength of 280 nm and the
 458 UV spectra of the morphological regions in three tissue fractions. Scl: sclerenchyma,
 459 V: vessel, S: sieve tube, F: fiber, P: parenchyma, CW: cell wall, ML_{CC}: middle
 460 lamella at a cell corner